Expanded View Figures

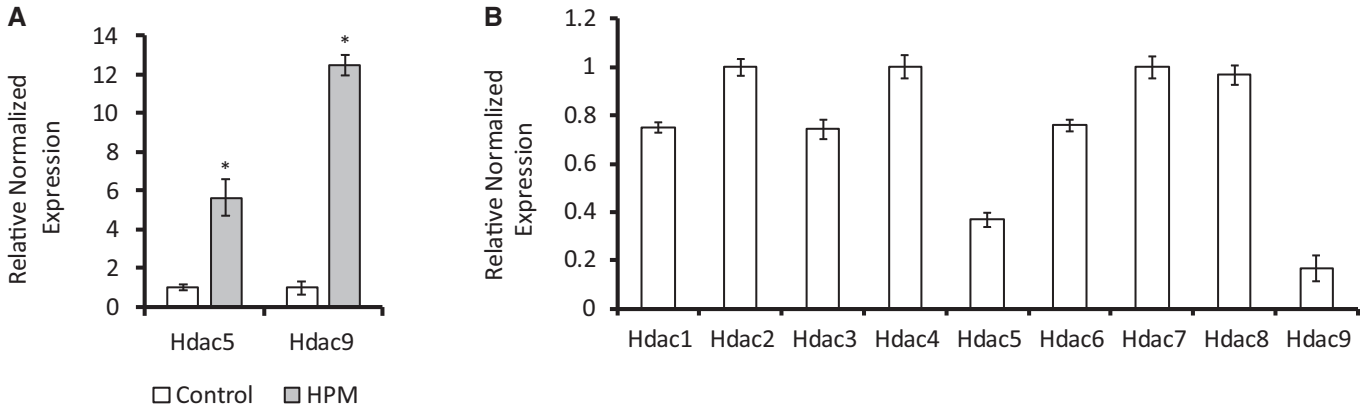

Figure EV1. HDACs expression levels in VSMCs.

A Gene expression qRT–PCR analysis of HDAC5 and HDAC9 in VSMCs following treatment with high phosphate media (HPM) (gray) or control media (white). Data are shown as means ± SEM (n = 6), normalized to control, with two-tailed unpaired Student's t-test, *$P < 0.05$.

B Expression levels of HDACs 1–9 in VSMCs grown in control media analyzed using qRT–PCR. Data are shown as means ± SEM (n = 6), relative to zero.

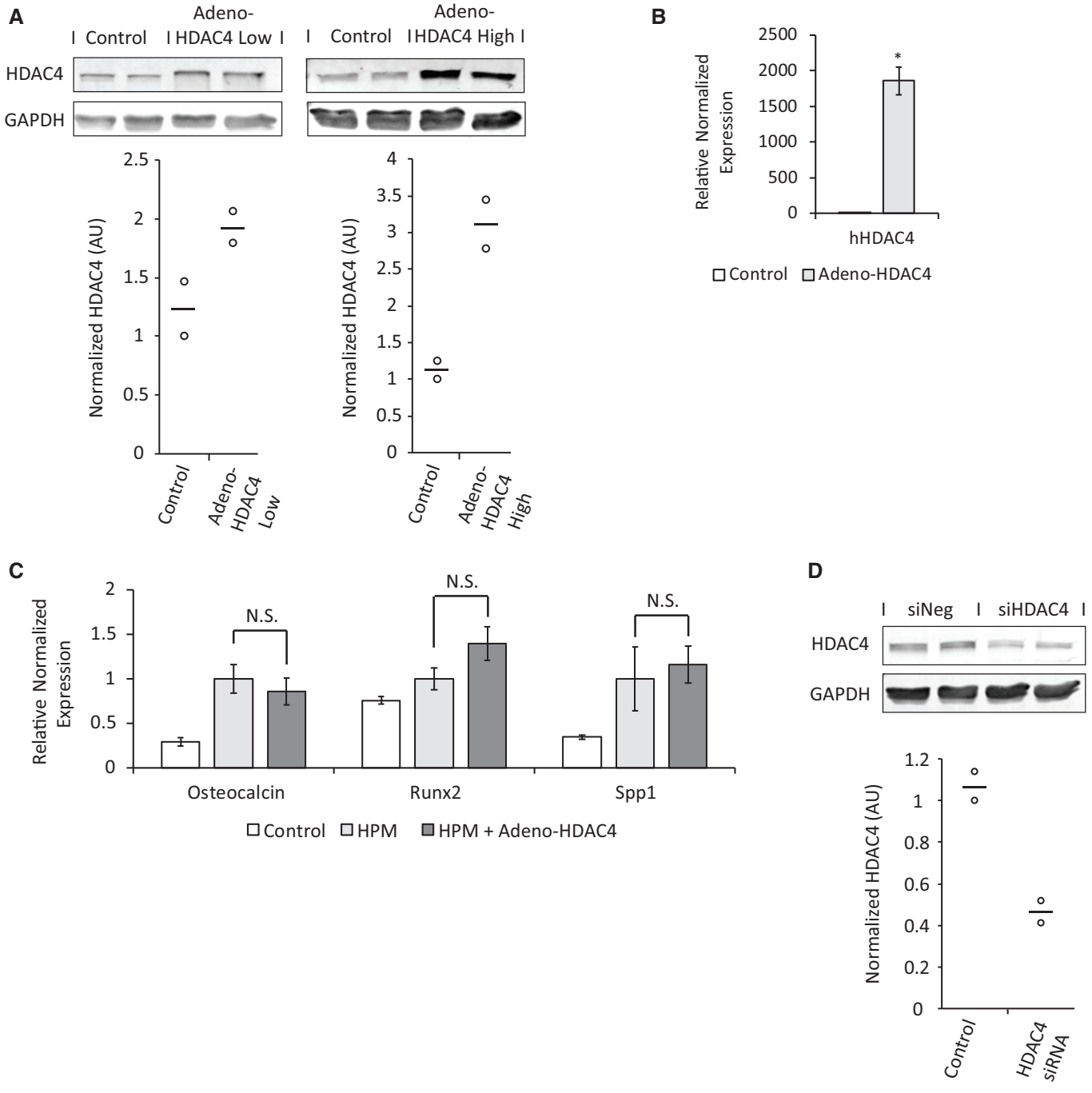

Figure EV2. Degree of HDAC4 knockdown and overexpression.

A Western blot analysis and quantification showing the degree of HDAC4 protein overexpression after viral transduction in VSMCs. Data are shown as single data points and mean (n = 2).

B qRT–PCR with human-specific HDAC4 primers in aortic rings showing effective viral transduction of Ad-HDAC4. This analysis, however, cannot be used to quantify the degree (fold-ratio) of HDAC4 overexpression over endogenous mouse HDAC4, since the level of human HDAC4 in control rings is zero. Data are shown as means ± SEM (n = 6), normalized to control. Two-tailed unpaired Student's t-test, $^*P < 0.05$.

C Aortic rings were transduced with adenoviral vector encoding for Flag-tagged HDAC4 or control beta-gal and were grown in HPM or control media. Gene expression qRT–PCR analysis for osteochondrogenic markers was performed. Data are shown as means ± SEM (n = 4), relative to zero. Two-tailed unpaired Student's t-test. N.S., $P > 0.05$.

D Western blot analysis and quantification showing the degree of HDAC4 protein knockdown in VSMCs in response to HDAC4 siRNA transfection. Data are shown as single data points and mean (n = 2).

Source data are available online for this figure.

Figure EV3. HDAC4 constructs and localization in HeLa cells.

A GFP-tagged constructs of HDAC4: Wild-type, full-length HDAC4 protein; 3SA, full-length HDAC4 protein, in which three amino acids (Ser^{246}, Ser^{467}, and Ser^{632}) were mutated to alanine; 3–625, the N-terminal fragment of HDAC4-containing amino acids 3-625 of the protein that includes the NLS but not the NES.

B HeLa cells were transfected with the different HDAC4 constructs to examine their intracellular localization. Cells were fixed with formaldehyde, and nuclei were counterstained with DAPI. High magnification representative images are shown. Scale bar = 10 μm.

C VSMCs were transduced with adenoviral vector encoding for Flag-tagged HDAC4 or Flag-tagged 3SA HDAC4. Cytoplasmic and nuclear protein extracts were obtained and Western blot was performed using anti-Flag antibody. Anti-tubulin immunoblot was used as a loading control and to mark the cytoplasmic fraction.

Source data are available online for this figure.

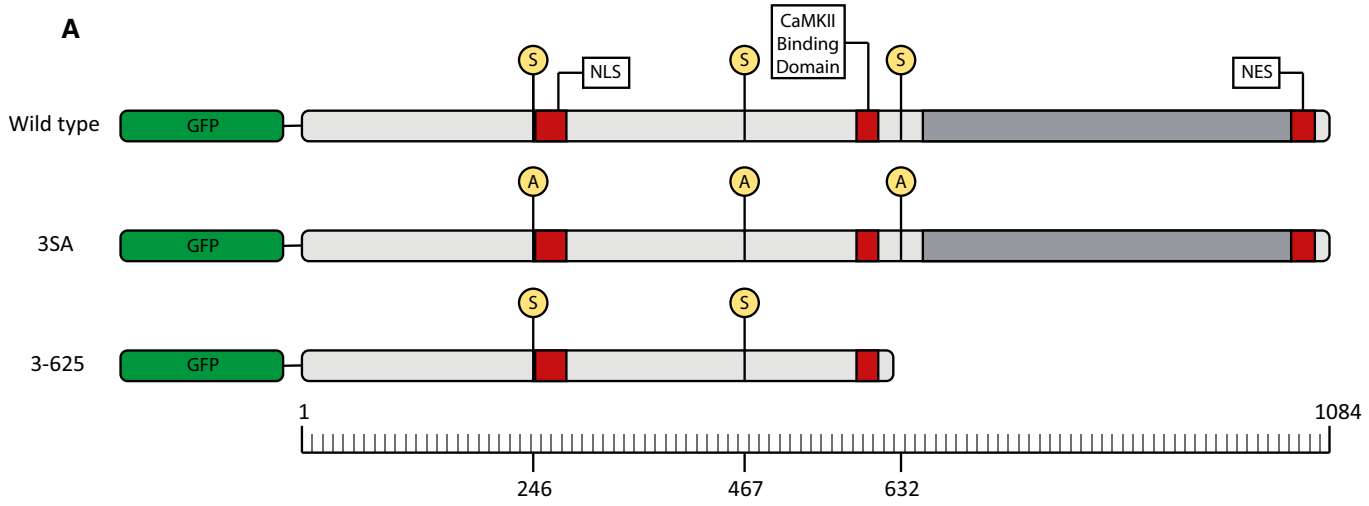

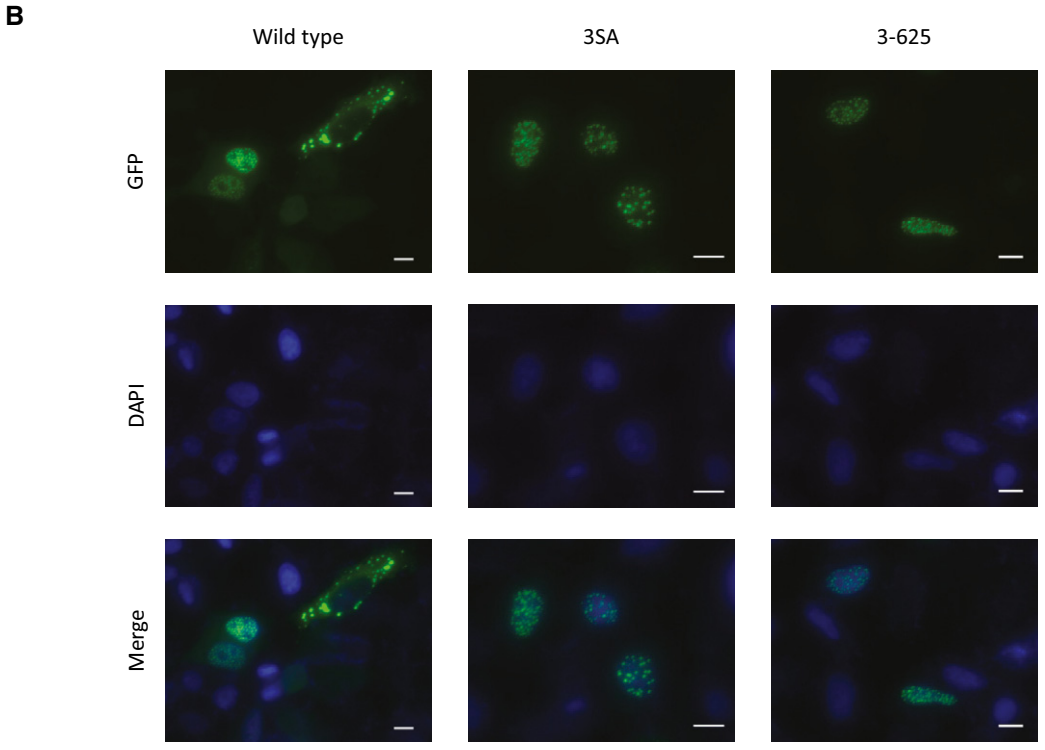

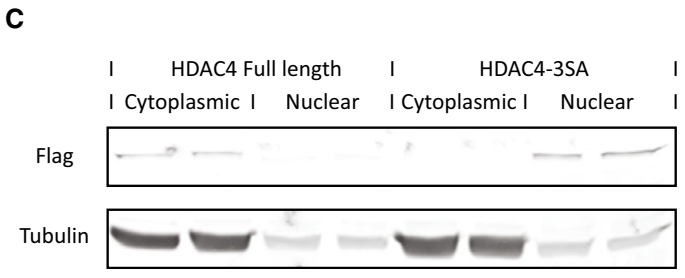

Figure EV3.

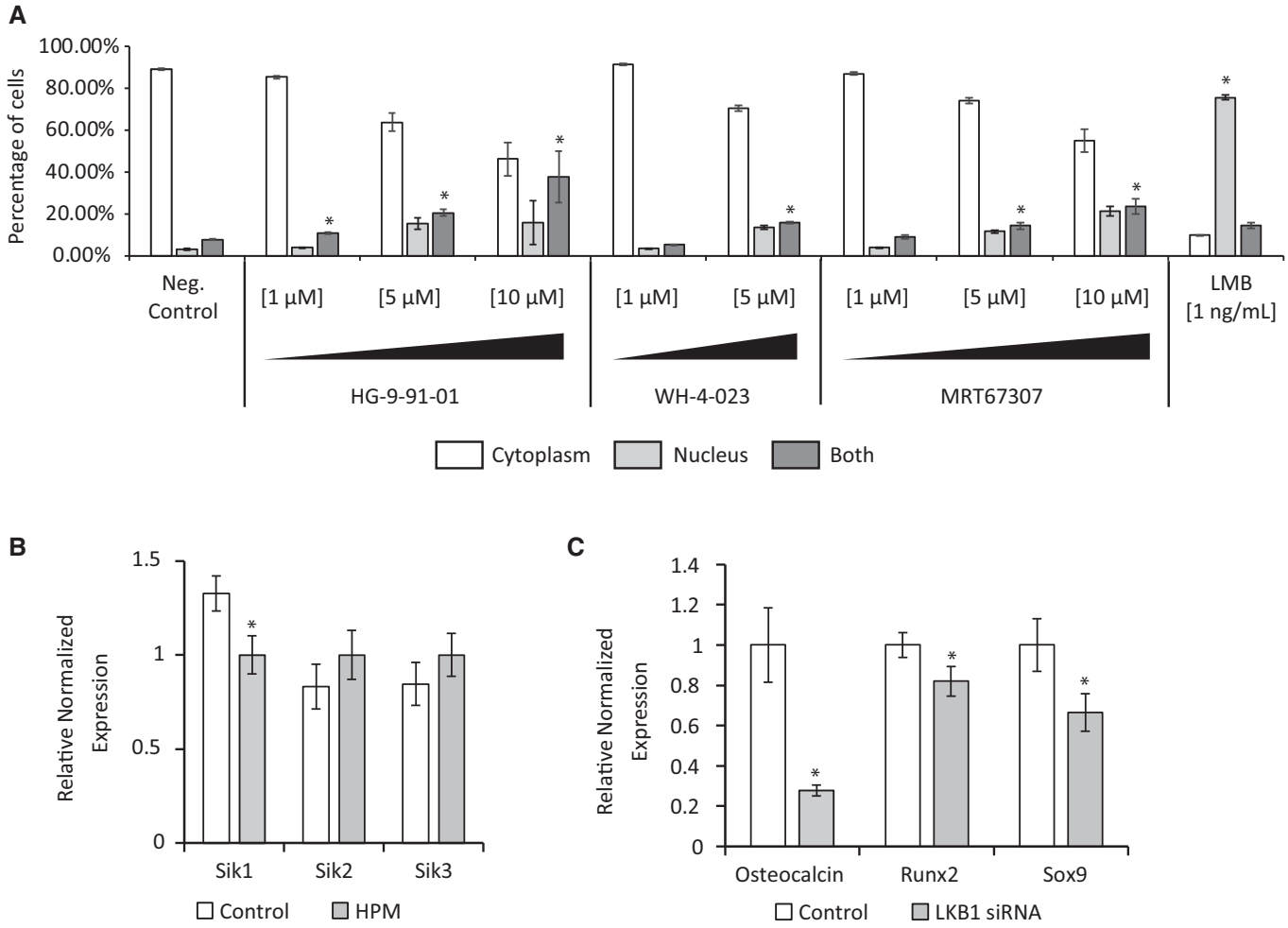

Figure EV4. Different SIK inhibitors control HDAC4 localization.

A GFP-HDAC4 localization after treatment with the indicated SIK inhibitors and concentration was scored automatically as being exclusively cytoplasmic (white), exclusively nuclear (light gray) or as occupying both a cytoplasmic and nuclear localization (dark gray) using CellProfiler cell image and analysis software [22]. All three pan-SIK inhibitors induced dose-dependent nuclear accumulation of HDAC4. Data are shown as means ± SD (n = 275 cells at least in each group). Chi-square proportion test, *$P < 0.001$.

B Gene expression qRT–PCR analysis of the three SIK isoforms in VSMCs shows modest downregulation of SIK1 and modest upregulation of SIK2 and SIK3 following treatment with HPM (gray). Data are shown as means ± SEM (n = 4), relative to control. Two-tailed unpaired Student's t-test, *$P < 0.05$.

C Gene expression qRT–PCR analysis of VSMCs transfected with control or LKB1 siRNA and grown in HPM for 7 days. Data are shown as means ± SEM (n = 4), normalized to control. Two-tailed unpaired Student's t-test, *$P < 0.05$.

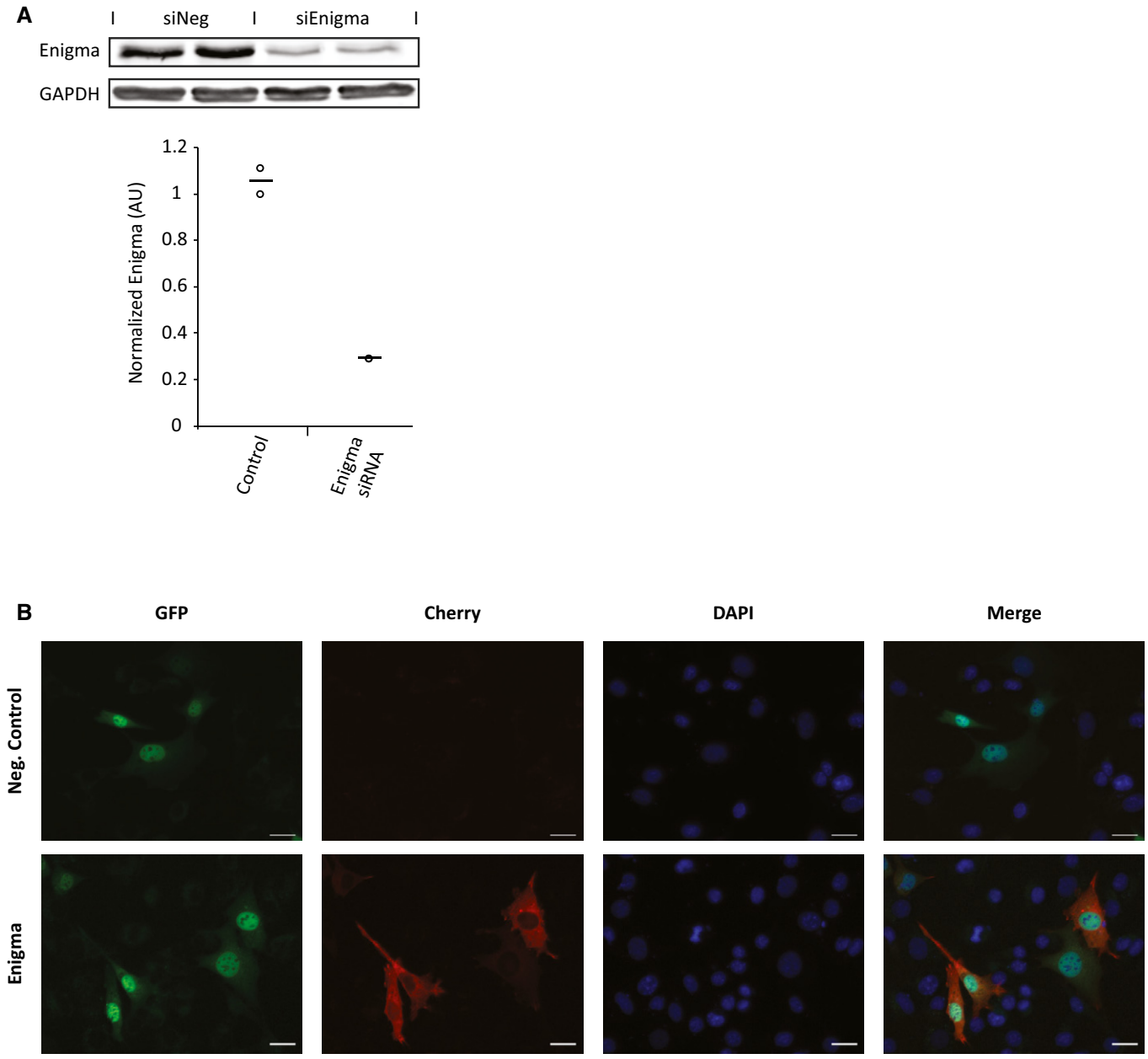

Figure EV5. Enigma knockdown and overexpression.

A Western blot analysis and quantification showing the degree of ENIGMA protein knockdown in VSMCs in response to ENIGMA siRNA transfection. Data are shown as single data points and mean (n = 2).

B VSMCs were co-transfected with GFP-3SA HDAC4 and Cherry-ENIGMA plasmids to observe whether ENIGMA overexpression can force cytoplasmic localization of 3SA HDAC4. Representative images are shown. Scale bar = 10 μm.

Source data are available online for this figure.

Figure EV6. ENIGMA binds the cytoskeletal proteins α-actinin and palladin and affects gene expression through the LINC complex.

A Cartoon of the α-actinin protein with its known structural domains. Four independent α-actinin clones, B1, B5, B8, and B11 (gray), were found to bind ENIGMA PDZ domain using the yeast Ras recruitment system (RRS). All clones contained the C-terminal domain of α-actinin.

B Cartoon of the palladin protein with its known structural domains. One clone, B2 (gray), was found to bind ENIGMA through its C-terminal domain, using the yeast Ras recruitment system (RRS).

C Expression from the bait plasmid is induced in media without methionine (-M), while expression from the prey plasmid is induced by galactose containing media (GAL). All five positive clones conferred growth at 36°C, only when the expression from both bait and prey plasmid was turned on (GAL-MUL media), indicating true interaction.

D VSMCs were transfected with SUN2 siRNA or control scrambled siRNA, and Osteocalcin levels were analyzed by qRT–PCR. Data are shown as means ± SEM (n = 4), normalized to control. Two-tailed unpaired Student's t-test, $^{*}P < 0.05$ vs. control, $^{\dagger}P < 0.05$ vs. HPM.

E Wild-type VSMCs were fixed with formaldehyde, immunostained with an anti-HDAC4 antibody (green), phalloidin (red), and nuclei were counterstained with DAPI (blue). Representative images are shown. Scale bar = 10 μm.

Source data are available online for this figure.

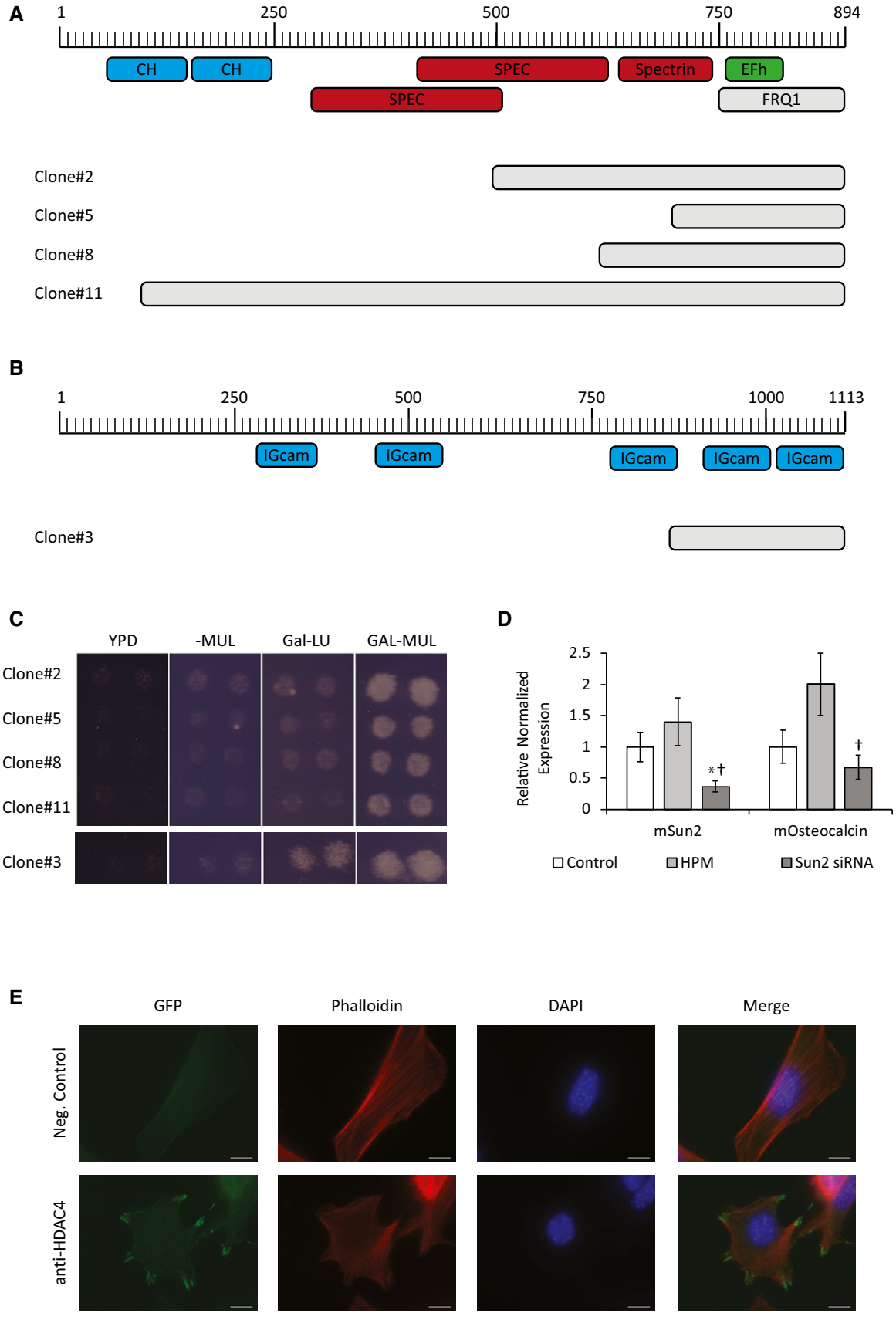

Figure EV6.